Journal of Rare Cardiovascular Diseases
ISSN: 2299-3711 (Print) | e-ISSN: 2300-5505 (Online)
www.jrcd.eu
RESEARCH ARTICLE

MACHINE LEARNING-BASED ENSEMBLE FOREST BOOSTED CLASSIFIER FOR CHARACTERIZING THE FETAL ANAMOLY BASED ON NUCHAL TRANSLUCENCY

Kavyashree Nagarajaiah[1], Ooi Chee Pun[2], Tan Wooi Haw [3]
[1]Assistant Professor, Department of MCA, Sri Siddhartha Institute of Technology, Tumkur, Karnataka, India.
[2] Ooi Chee Pun, Associate Professor, Multimedia University, Cyberjaya, Malaysia
[3]Tan Wooi Haw, Associate Professor, Multimedia University, Cyberjaya, Malaysia

*Corresponding Author

Article History
Received: 01.09.2025
Revised: 15.09.2025
Accepted: 30.09.2025
Published: 08.10.2025

Abstract: *An ultrasound scan in the mid-trimester has become a routine part of antenatal care in most mat*ernity hospitals. As technology progresses and scanning capabilities enhance, the identification of foetal abnormalities in scans is on the rise. Foetal anomalies refer to developmental abnormalities that arise in a foetus during the course of pregnancy. Birth defects and congenital abnormalities are terms that are interconnected. In recent decades, industrialised nations have consistently reported cases of foetal abnormalities. Three out of every 1,000 expectant women experience a foetal anomaly. This study proposes an ensemble forest-boosted algorithm to evaluate the risk of foetal abnormalities through the analysis of nuchal translucency (NT). The data was retrieved initially here. Subsequently, it can be processed with the colab mean filter. The region of interest can subsequently be delineated through the application of the iterative coarse-grained seed algorithm (ICGSA). The ensemble forest boosted classifier (EFBC) was ultimately implemented to identify foetal anomalies. The findings of this work indicate that the proposed innovative method can effectively classify the anomalies associated with nuchal translucency thickening. The analysis includes parameters such as accuracy, recall, precision, and F1-score. The technique proposed yields an accuracy of 99.642%. Index Terms— Fetal abnormality, iterative coarse-grained seed algorithm, ensemble forest boosted classifier.

Keywords:

INTRODUCTION

Down syndrome (DS), also known as trisomy 21, affects about 1 in 700 newborns. This hereditary condition is very dangerous. In Down syndrome, chromosome 21 has three copies, one of which is an extra gene. Typically, there are two copies of every chromosome. This hereditary disorder is caused by an extra 21st chromosome. The disorder's modest to severe symptoms may have an influence on both cognitive and physical development. Having Down syndrome could cause significant differences in a person's physical traits, health problems, and cognitive development. Multiple prenatal and postnatal screenings and tests may diagnose DS. There are other outward differences between a DS foetus and a euploid foetus, such as a different font-maxillary (FMF) angle, a bigger nuchal translucency, and the lack of a nasal bone [1]. During the first trimester of pregnancy, trained professionals use ultrasound scans to determine the NT thickness.
(See Figure 1) .

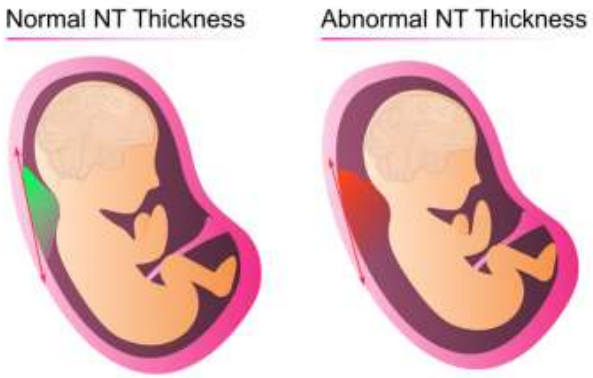

Figure 1 Fetal normal and abnormal NT projection

Measurements of NT thickness[4-6] conducted in the first trimester of pregnancy may be able to identify chromosomal abnormalities in the developing foetus (See Table 1).

Table I. NT Thickness and the Frequency of Chromosomal Problems

	"Nuchal Translucency	Major Foetal Abnormalities [10]	Foetal Death [10]	Chromosomal Defects [2] [AI_2]
I	> 6.50 mm	46.20%	19.00%	64.50%
2	5.5 – 6.40 mm	24.20%	10.10%	50.50%
3	4.5 – 5.4 mm	18.50%	3.40%	33.30%
4	3.5 – 4.4 mm	10.00%	2.70%	21.10%
5	95 th-99th centiles	2.50%	1.30%	3.70%
6	< 95 th centile	1.60%	1.30%	0.20%"

Both typical and abnormal growth may be detected by using the population-based growth chart. When evaluating foetal parameters manually, there is both inter- and intraobserver variability [7]. There is less variation and higher precision and repeatability in the measurements of foetal parameters when they are done automatically. Automated foetal monitoring technologies improve efficiency and provide more accurate readings of foetal traits. Though it might lead to inaccuracy, the radiologist can determine the foetal condition by precisely assessing these features. Therefore, anomaly prediction using computer aids relies on AI-based mechanisms. This study used an innovative method for predicting foetal abnormalities: an ensemble forest-boosted classifier. All things considered, the work's contribution comprises,

- Implementation of the novel segmentation methodology for identifying the region of interest
- To identify the abnormality in the fetus based on the NT using the ensemble forest boosted classifier.

The remainder of this work is broken down into the following sections: The second part is a review of related research. The third portion focuses on the study's methodology. The fourth section evaluates the suggested methodology performance. In the last chapter, the findings of the study are presented, examined, and discussed.

Related Works

Some instances of scientific articles that have addressed abnormalities in the developing foetus are as follows. Prenatal ultrasonography is a valuable technique for detecting congenital abnormalities, detecting aneuploidy, and monitoring the baby's development. Here is a survey of the literature from 2021 onward that focuses on fetal anomaly prediction using deep learning techniques, based on recent studies and reviews.

[1] discusses the development of a novel deep learning model, the Multi-Feature Pyramid U-Net (MFP-U-Net), for automatic fetal biometry prediction. The model was designed to accurately segment and predict key fetal anatomical parameters such as head circumference, abdominal circumference, and femur length from ultrasound images. The model uses attention gates to focus on relevant structures while ignoring irrelevant features, improving both sensitivity and accuracy. The research demonstrates the potential of deep learning in automating fetal anomaly detection by achieving high precision in ultrasound imaging segmentation

.

A deep hybrid learning method was introduced to classify fetal brain abnormalities using MRI and ultrasound data. The study [2] integrated convolutional neural networks (CNN) with long short-term memory (LSTM) networks to capture both spatial and temporal features in fetal brain images. This hybrid model was particularly effective in detecting structural abnormalities like hydrocephalus and microcephaly, offering insights into how deep learning can assist in identifying complex fetal conditions.

[3] critically analyzes various machine learning and deep learning algorithms applied to fetal ultrasound images. The paper discusses the challenges in ultrasound imaging, such as low resolution and artifacts, and evaluates the efficacy of different models like CNN, U-Net, and transfer learning for fetal anomaly detection. The authors emphasize the importance of creating models that not only improve detection accuracy but also enhance the clinical usability of automated systems. **[4]** focused on fetal kidney abnormalities, CNNs were used to classify renal defects from ultrasound scans. The model was trained to identify conditions like hydronephrosis and polycystic kidney disease. This research highlights the potential of deep learning in automating the analysis of kidney abnormalities, which are often difficult to diagnose manually

[5] combined CNNs for image feature extraction with LSTMs for sequential data analysis. The model was used to detect a variety of fetal anomalies from both ultrasound and MRI scans. The study showed that hybrid models could effectively capture both spatial and temporal patterns, leading to better anomaly detection compared to traditional CNN-based methods

[6] proposed an innovative approach that uses LeNet to detect structural anomalies in the fetal brain. Their model, based on a large dataset of ultrasound images, focuses on the early identification of conditions such as hydrocephalus and neural tube

defects. By applying transfer learning from pre-trained models, their approach achieved an accuracy of 92%, which is a significant improvement over traditional methods

[7] the study emphasizes the clinical significance of accurate diagnostics, detailing the training and validation process of the AI model, ensuring ethical considerations, and highlighting the potential of the model in real-world clinical settings. By pushing the boundaries of current diagnostic capabilities and emphasizing rigorous clinical validation, this research work aims to contribute significantly to medical imaging and pave the way for more precise and reliable fetal health assessments.[8] proposed the transverse dyadic wavelet transform algorithm to retain the border and curvature of four chambers on foetal cardiac ultrasound images. [9] proposed neural network-based prenatal detection of complicated CHD. In this detection, a view classifier categorised the ultrasound view, and then three CHD diseases could be detected independently by successive detection classifiers. [10] proposed a convolutional neural network to detect cardiac substructures and structural abnormalities on foetal ultrasound videos. This detection method only adopted a supervised learning scheme from a dataset of normal cases[11] and proposed an AI-based method for segmenting anatomical structures in the foetal apical four-chamber view. They divided a MobileNet backbone network into four stages and designed an FPN network to enhance multi-scale semantic information.

Current methods [12,13,14,15] do a better job of assessing foetal hazards, but they might be much better if they were more efficient. Here, we used a new EFBC method to categorise foetal anomalies as either low-risk or high-risk.

PROPOSED WORK

The recommended procedure for detecting foetal abnormalities is this. Processing of NT for the purpose of diagnosing foetal abnormalities is described in this article. Figure 2 depicts the schematic of the proposed methodology's overall operation.

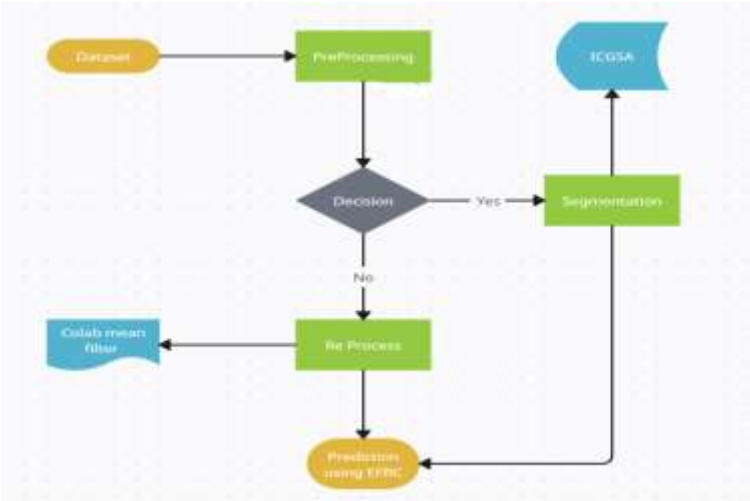

Figure 2 Schematic representation of the suggested methodology

a.Dataset

The Mediscan Foetal Care Research Foundation in Chennai, India, supplied the US foetal imaging. Among the 100 foetuses included in the sample were those in the 11–14 week gestational range. In the database, you can find 50 DS foetuses and 50 healthy ones. The image dimensions are 1136 by 852 pixels. The Foetal Medicine Foundation (FMF) laid out the necessary steps for precise NT assessment. The doctor additionally recorded the mother's age and crown-rump length in the dataset [40].

b.Data processing

Image quality, size variance, and inherent noise are issues with US Images. The active image quality is diminished by speckles, which is granular noise seen in US images. Removing noise and deformed pixels is an important first step in image processing, which allows us to recover valuable features from the images. Prior to processing, the US image undergoes operations including resizing and filtering. Filtering improves the image quality, sharpens the edges, and decreases noise. Using a colab mean filter, an image may be filtered.

Step A: Equation (1) is used to build a synthetic instance.

$$N = 2 * (r - z) + z\#(1)$$

This means that r represents samples from the majority class, z represents samples from the minority class, and N represents a freshly produced synthetic instance.

Step B: To eliminate the outlier or backdrop, use these techniques.

Noise:

The acquisition of a new instance via Step A

$\dot{S} = \{\dot{S}_1, \dot{S}_2, \dot{S}_3, \ldots . \dot{S}_n\}$, we will use Equation (2) to determine the distance between $\dot{S}_i$ and the original minority S_m, Min $n_{\text{Rap}}(\dot{S}_i, \dot{S}_m)$.

$$\text{Min}_{\text{Rap}}\ (\dot{S}_i, \dot{S}_m) = \sum_{k=1}^{z} \sum_{j=1}^{M} \sqrt{\left(\dot{S}_i^{(j)} - S_{mk}(j)\right)^2}\#(2)$$

where

$\text{Min}_{\text{Rap}}\ (\dot{S}_i, \dot{S}_m) \rightarrow$ The closeness of the samples and Equation (3) are used to compute L (EQU2).

$$L = \sum_{i=1}^{n} \left(\text{Min}_{\text{Rap}}\ (\dot{S}_i, S_m)\right)\#(3)$$

Step C: The distance between each initial majority , Maj Rap $(\dot{S}_i, S_a)s$, as specified by Equation (4), and all $\dot{S}_i$, must be calculated.

$$\text{Maj}_{\text{Rap}}\ (\dot{S}_i, S_a) = \sum_{i=1}^{r} \sum_{j=1}^{M} \sqrt{\left(\dot{S}_i^{(j)} - S_{al}^{(j)}\right)^2}\#(4)$$

$\text{Maj}_{\text{Rap}}(\dot{S}_i, S_a) \rightarrow$ H is determined by using Equation (5) in conjunction with the sample convergence and Equation (4).

$$H = \sum_{i=1}^{n} \left(\text{Maj}_{\text{Rap}}\ (\dot{S}_i, S_a)\right)\#(5)$$

Chaos may be quantified using just entropy. Claude E. Shannon demonstrated the relationship between heterogeneity and probability using equations (6) and (7).

$$H(X) = -\sum\ (p_i * \log_2\ p_i)\#(6)$$

$$\text{Entropy (p)} = -\sum_{i=1}^{N} p_i \log_2\ p_i\#(7)$$

The likelihood of eradicating the mistake occurrences is a key factor.

Therefore, in order to prevent the impact of image size on system performance, the pre-processing procedure helps to normalise every image such that they are independent of their source.

c.Segmentation

The recommended method used an iterative coarse-grained seed mechanism to first segment the ROI. Clustering is used to initialise the seed function to a value in the proposed approach. The technique causes the image to have deceptive blobs and extremes. In order to separate these extraneous effects, we use Gaussian filtering. The next thing to do is to initialise the ROI function using the feature clustering findings.

$\mathcal{M}_{i,j} =$ feature Membership Function

$\mathcal{Z}_{i,j} =$ ROI extracted from image

A ROI is computed using,

$$\mathcal{Z}_{i,j} = \begin{cases} 1, & u_{ij} > b_0 \\ 0, & \text{otherwise} \end{cases}$$

$b_0 \in (0,1)$ is adjustable threshold

The coarse-grained function is set up initially as:

$$\varphi_0(x, y) = 2\varepsilon(2\mathcal{Z}_{i,j} - 1)\#(8)$$

$\varepsilon =$ constant meant for regularizing the Dirac function

Conventional methods include manually inputting values for regulating parameters to affect the level-set function's development; these values change based on the application. The proposed method adaptively evaluates all the required regulating parameters using the segmentation results. To measure the area and length of the feature clustering-generated contour, the Heaviside and Dirac functions are used.

$$\mathcal{C}_{\text{Area}}(\varphi \geq 0) = \int_{-\Omega}^{\Omega} \mathcal{H}(\varphi(x,y))dxdy \#(9)$$

$$\mathcal{C}_{\text{Length}}(\varphi = 0) = \int_{-\Omega}^{\Omega} \delta_0(\varphi(x,y))|\nabla\varphi(x,y)|dxdy \#(10)$$

Here, the Heaviside function may be described as:

$$\mathcal{H}(\varphi) = \begin{cases} 1, & \text{if } \varphi \geq 0 \\ 0, & \text{if } \varphi < 0 \end{cases} \#(11)$$

and the Dirac function as:

$$\delta_0(\varphi) = \frac{d}{d\varphi}\mathcal{H}(\varphi) \#(12)$$

This means that in the suggested technique, the value of m is calculated based on the output of the segmentation as:

$$v = 0.5 - u_{i,j} \#(13)$$

$_{\text{UI},j}$ = membership function associated with segmentation for every pixel

d.Prediction

One way to classify the EFBC technique is as an ensemble learning strategy. This research aimed to build a classifier model for attack data classification using the Ensemble approach and the Random Forest methodology. The EFBC classifier model is built utilising several RF classifiers. Without affecting one another, the classifier allows for the training and testing of models to happen simultaneously. A g-component training dataset G was used for this study.

$H = h_1, h_2, \ldots, h_p$ (14)

The input customization features are denoted as $R_1, R_2, \ldots, R_n$, where n represents the total number of parameters for customization features

$H \in R^{m \times r}$ (15)

The formulation of the EFBC representation of an element g in a tree s may be expressed as:

$f_s(h) = f(h, \theta_s)$ (16)

Where $\theta_s$is the input vector of h is linked to a vector that is created randomly.

To accurately classify a given sample g into class v using the EFBC technique, the probability is represented by Equation (16). The mathematical formula for the margin function associated with this prediction is given by equation (17). To measure how many votes each properly identified category received on average in comparison to all other categories, statisticians utilise the margin function. For the random forest method to provide its output, the decision function, denoted as (18), must be invoked.

$P(v \mid h) = \frac{1}{S}\sum_{s=1}^{S} P_s(v \mid h)$ (17)

The notation P(v■g) represents the anticipated probability density of class labels for a given sample g inside a certain collection of trees. S represents the sum of all the trees found in the forest.

$mh(h, v) = P(v \mid h) - \max P(j \mid h)$ (18)

where $j \in w; j \neq v$; For values of (18) > 0, There is a higher probability that the classifier will accurately forecast the abnormality classifications.

The abnormal categories or classes, labelled as $cl_1, cl_2, \ldots, cl;$, correspond to the total count of NT

$f_n: S_1, S_2, \ldots, S_n \mapsto B_1, B_2, \ldots, B_n; B_i \in \mathbb{R}; n \in \mathbb{N} h_n: x = \{(R_1, R_2, \ldots, R_n) U(B_1, B_2, \ldots, B_{n;})\} \mapsto y$ (19)

$y \in \{cl_1, cl_2, \ldots, cl_p\}; \quad p \in \mathbb{N}/0,1$ (20)

$\rho_{\text{class}} = f_n U h_n$ (21)

Finally, the NT abnormality data can be classified.

Performance Analysis

The first stage was to sort the datasets into "train" and "test" categories. We were able to gauge the success of our suggestion by using this method. For each trial, Python was the preferred platform. Experiment hardware included a GeForce RTX 2080 Ti GPU and an Intel (R) Xeon (R) Gold 5220 CPU, and the pytorch framework was used for training.

Figure 3 Sample input

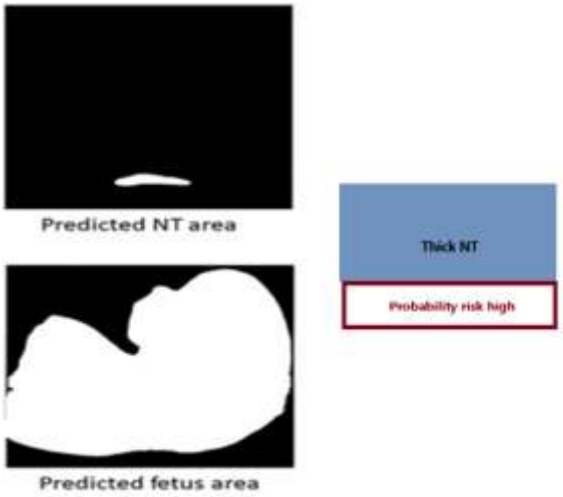

Figure 4 Simulated output

The sample input and the simulated output are illustrated in Figure 3,4

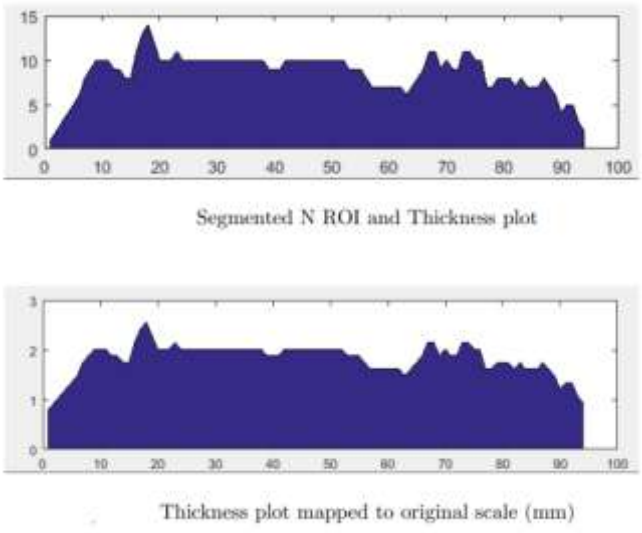

Figure 5 Thickness plot analysis

Figure 5 displays the results of the NT ROI segmentation. The red colour is used to indicate the NT area. To determine the thickness of the NT, vertical pixel counting is performed after obtaining the segmented ROI. The NT ROI pixels are shown on the X-axis, and their pixel count, which represents our NT thickness in pixels, is shown on the y-axis. After the pixel count is obtained, the original scale is restored by using the reference chart of pixels to millimetres that are included in the classifier.

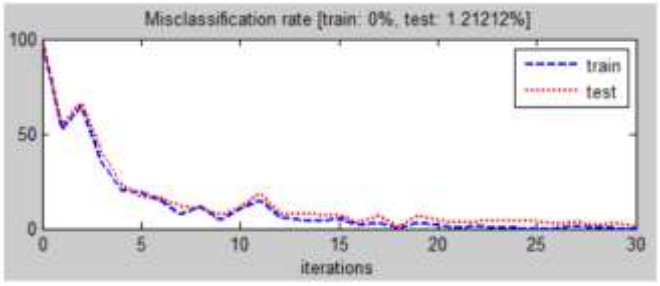

Figure 6 Misclassification rate analysis

The misclassification rate is a performance metric for the design that allows us to examine the outcomes. The rate at which samples are incorrectly classified is called the misclassification rate. For every session, thirty iterations were run across the whole training data set. For 434 test data and 750 training data, the resultant misclassification rate is 1.21%, as shown in Figure 6. So, out of 428 data samples, the proposed model got 6 right and 6 wrong.

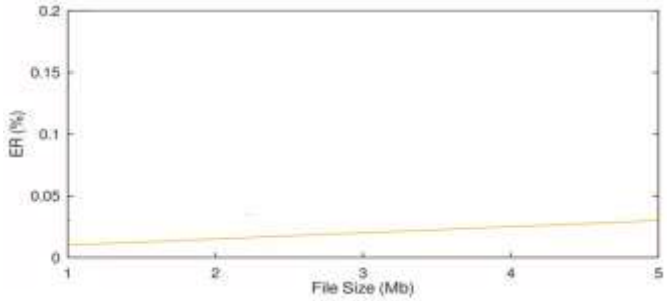

Figure 7. Error rate analysis

Figure 7 shows the error rate was less (0.03%) for the suggested methodology.

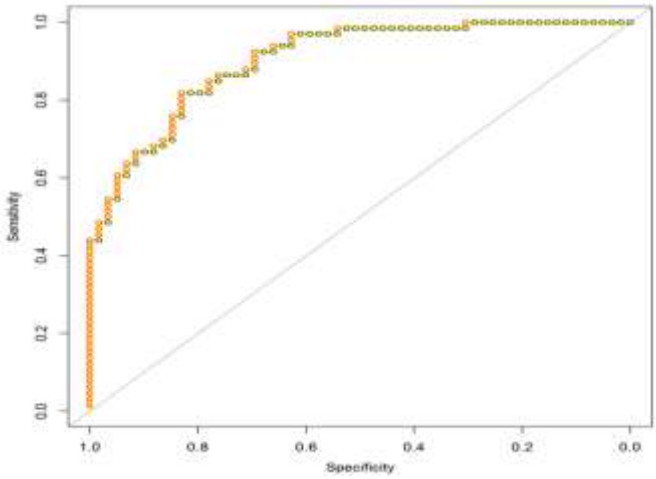

Figure 8 Analysis of AUC

The AUC curve on fetal anomaly data in Figure 8 represents that the suggested methods show an outstanding value of AUC (99)%.

Accuracy, Precision, Recall, and F1-score are some performance metrics that may be used to assess how well the classification process is working.

Accuracy: The accuracy of a model in a classification task is defined as the percentage of accurate predictions relative to all potential predictions. A hundred is the result of multiplying the sum of all guesses by the number of correct predictions.

$$\text{Accuracy} = \frac{\square_{\square}+\square_{\square}}{\square_{\square}+\square_{\square}+\square_{\square}+\square_{\square}}. \quad (22)$$

Precision: Precision is the ratio of true positives and total positives predicted.

$$\text{Precision} = \frac{\square_{\square}}{\square_{\square}+\square_{\square}}. \quad (23)$$

The accuracy of a diagnosis of brain tumour is determined by the percentage of the foetus that really exhibited the anomaly.

Recall: The proportion of correct predictions to total predictions in the baseline data is called recall.

$$\text{Recall} = \frac{\square_{\square}}{\square_{\square}+\square_{\square}}. \quad (24)$$

F1-score: The F1-score measures both recall and accuracy. Actually, averaging the two harmonics yields the F1 score. Having a high F1 score means that your memory and accuracy are both excellent.

$$\square_1 = \frac{2}{\frac{1}{\text{Precision}} + \frac{1}{\text{Recall}}} \#(25)$$

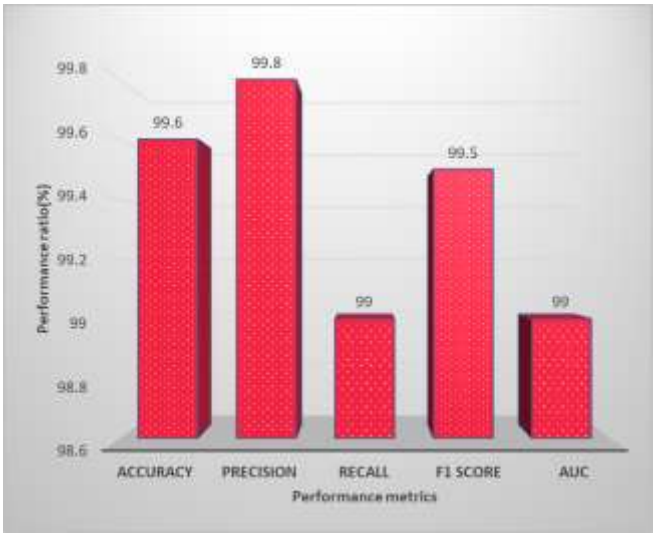

Figure 9 Performance analysis of the suggested methodology

Figure 9 shows that the proposed technique achieved satisfactory results in brain tumour prediction, with a range of 99% for recall, 99.8% for precision, and 99.5% for f score.

Table 2 Error Between Measured and Automatic NT Thickness Measurements (Maximum)

Method	Measured Maximum NT Thickness in mm	Automatic Maximum NT Thickness in mm	Error in mm
MRF[15]	2.930	2.90	0.03
SegNet19[15]	2.930	2.70	0.23
GRNN11[15]	2.930	2.840	0.09
RBED18[15]	2.930	2.70	0.23
HSM17[15]	2.930	2.480	0.45
proposed	2.93	2.89	0.03

Table 2 displays the maximum error between the measured and automatic NT thickness readings. This demonstrates that, in comparison to manual measurement, the proposed method's margin of error is lower.

An analysis of the research on foetal abnormality identification has been conducted thus far. The application domain, number of images, critical performance indicators, and methodologies used are all detailed in each entry.

The results shown in Table 2 indicate that the suggested method outperforms the already-used approaches. Hence, it is recommended to consider using a suggested classifier in order to get good results when using this dataset to predict the probability of fetal abnormality.

Table 3 Comparative performance analysis

"Method	Total Images	Metrics	Application
GACNN + DANomaly	3196	85.00%	Detection of heart defects
Ensemble of NN	107,823	AUC: 99%	Detection of heart defects
SOLOv2 + CAM	319	DICE: 74.70–81.99%	Segmentation of cardiac four-chamber view
U-Net + FCN	312	Heart: DICE: 90.2% IoU: 0.822 Lung: DICE: 87.00% IoU: 0.770	Segmentation of views of the lung and heart
Mask-RCNN	1149	DICE: 89.70% IoU: 79.97%	Detection of heart defects
Cascaded DW-Net	895	DICE: 82.7%	Segmentation of cardiac four-chamber view
U-Net + FPN	Original: 137 Augmented: 1370	Average DSC: 95.3%	Segmentation of cardiac four-chamber view
YOLOv5	1779	Overall accuracy: 90.67%	Detection of ventricular septal defects
CNN + D-CNN + ARVBNet	Original: 7032 Augmented: 12,542	MAP: 93.52%	Fetal heart image quality control system
U-Net + ResNet	740	DICE: 91%	Detection of fetal brain anomalies
SVM Classifier	86	Accuracy: 87.10%	Classify fetal head US images
YOLOv3	43,890	AUC: 89.8–98.1%	Diagnose congenital CNS malformations
DenseNet	289	Overall accuracy: 93%	Detection of cystic hygroma
GCN	Original: 1334 Augmented: 11,324	DICE: 98.21%	Fetal head circumference measurement
Lightweight-DCNN	Original: 1334 Augmented: 10,898	DICE: 97.61%	Fetal head circumference measurement
RUSBoost	295	Accuracy: 81.18%	Detection of lung abnormalities: NRM
SVM Classifier	548	Accuracy (independent test set): 80.6–86.4%	Detection of lung abnormalities: GDM/PE
Ensemble Learning	932	Sensitivity: 97%	Detection of trisomy 21, 19, 13
Adaptive Stochastic Gradient Descent	100	Precision: 98.64%	Detection of chromosomal anomalies using NT thickness
Nomogram	622	AUC: 98.3–97.9%	Detection of trisomy 21
Proposed	-	Accuracy 99.6%	Whole fetus"

Journal of Rare Cardiovascular Diseases
ISSN: 2299-3711 (Print) | e-ISSN: 2300-5505 (Online)
www.jrcd.eu
RESEARCH ARTICLE

CONCLUSION

In this study, we provide a new approach to early foetal anomaly detection that makes use of ML. In order to facilitate speedier calculation, the speckle noise in the foetal US image was preprocessed and the images were shrunk. Using the ICGSA architecture, the NT contours were semantically segregated from US foetal images, and the EFBC Model was used for successful classification. Clinicians will find the CAD to be an invaluable resource for screening for NT-based foetal anomalies since it increases the detection rate and offers a second view that may help with early diagnosis. In the future, the fetal anamoly can identified using chromosome or syndrome-related parameters".

REFERENCES

1. Oghli, M. G., Shabanzadeh, A., Moradi, S., Sirjani, N., Gerami, R., Ghaderi, P., ... & Zaidi, H. (2021). Automatic fetal biometry prediction using a novel deep convolutional network architecture. Physica Medica, 88, 127-137.
2. K. Shinde and A. Thakare, "Deep Hybrid Learning Method for Classification of Fetal Brain Abnormalities," 2021 International Conference on Artificial Intelligence and Machine Vision (AIMV), Gandhinagar, India, 2021, pp. 1-6, doi: 10.1109/AIMV53313.2021.9670994.
3. Shinde, K., & Thakare, A. (2021, September). Deep hybrid learning method for classification of fetal brain abnormalities. In 2021 International Conference on Artificial Intelligence and Machine

   Vision (AIMV) (pp. 1-6). IEEE.Ultrasonography Images: A Review of Machine Learning-Based Approaches. Biomimetics, 8(7), 519.
4. Yousefpour Shahrivar, R., Karami, F., & Karami, E. (2023). Enhancing Fetal Anomaly Detection in Ultrasonography Images: A Review of Machine Learning-Based Approaches. Biomimetics, 8(7), 519.
5. Patel, S. R., Madireddy, V. R., & Rajiv, K. (2024). Fetal Heart Abnormality Detection in Prior Stage Using LeNet 20 Deep Learning Architecture. Traitement du Signal, 41(4), 2103.
6. Mavaluru, D., Ravula, S. R., Auguskani, J. P. L., Dharmarajlu, S. M., Chellathurai, A., Ramakrishnan, J., ... & Ravishankar, N. (2024). Advancing Fetal Ultrasound Diagnostics: Innovative Methodologies for Improved Accuracy in Detecting Down Syndrome. Medical Engineering & Physics, 104132.
7. Liu, B., et al.: A denoising and enhancing method framework for 4D ultrasound images of human fetal heart. Quant. Imag. Med. Surg. 11(4), 1567–1585 (2021). https://doi.org/10.21037/qims-20-818
8. Arnaout, R., et al.: An ensemble of neural networks provides expert-level prenatal detection of complex congenital heart disease. Nat. Med. 27(5), 882–891 (2021). https://doi.org/10.1038/s41591-021-01342-5
9. Pu, B., et al.: Mobileunet-fpn: a semantic segmentation model for fetal ultrasound four-chamber segmentation in edge computing environments. IEEE Journal of Biomedical and Health Informatics 26(11), 5540–5550 (2022). https://doi.org/10.1109/jbhi.2022.3182722
10. Chan, W.X., et al.: Full cardiac cycle asynchronous temporal compounding of 3d echocardiography images. Med. Image Anal. 74, 102229 (2021). https://doi.org/10.1016/j.media.2021.102229
11. Qiao, S., et al.: Flds: an intelligent feature learning detection system for visualizing medical images supporting fetal four-chamber views. IEEE Journal of Biomedical and Health Informatics 26, 4814–4825 (2022)
12. M. Komatsu et al., Detection of cardiac structural abnormalities in fetal ultrasound videos using deep learning, Applied Sciences, 11(1): 371, 2021, doi: 10.3390/app11010371.
13. A. Fukuda, C. Han, K. Hakamada, Effort-free automated skeletal abnormality detection of rat fetuses on whole-body micro-CT scans, [in] 2021 IEEE International Conference on Image Processing (ICIP), Anchorage, AK, USA, pp. 279–283, 2021, doi: 10.1109/ ICIP42928.2021.9506216.
14. Verma, D., & Agrawal, S. (2023). A Novel Framework for Fetal Nuchal Translucency Abnormality Detection Using Hybrid Maxpool Matrix Histogram Analysis. Computer-Assisted Methods in Engineering and Science
15. Chaudhari, K., & Oza, S. (2024). Measurement of Nuchal Translucency Thickness in First Trimester Ultrasound Foetal Images Using Markov Random Field. Journal of Pharmacology and Pharmacotherapeutics, 15(1), 46-53.